Density-functional approach to LCAO methods

F.J. García-Vidal, J. Merino, R. Pérez, R. Rincón, J. Ortega, and F. Flores
Departamento de Física de la Materia Condensada C-XII, Facultad de Ciencias, Universidad Autónoma de Madrid E-28049 Madrid, Spain
(Received 22 December 1993; revised manuscript received 6 May 1994)

A Kohn-Sham approach is presented for analyzing the many-body properties of LCAO Hamiltonians. The total electronic energy of the system is shown to be a function of the different orbital occupancies. Then an exchange-correlation potential is introduced for each orbital, taking into account extra-atomic and intra-atomic many-body effects. Using this potential, the total energy can be obtained by calculating self-consistently the orbital occupancies, avoiding the use of a local representation as is done in the conventional LDA calculations. The method is applied to the calculation of the chemisorption energy and the charge transfer for the deposition of Na on Al(100), and the interaction of H with the GaAs(110) surface. Hydrogen is shown to passivate GaAs(110) surfaces for a monolayer deposition.

I. INTRODUCTION

Density-functional theory[1–3] and mainly calculations based on its local-density (LD) approximation[1–5] are pervading solid state physics. This approach has received recently an important momentum from the *ab initio* molecular dynamics scheme.[6]

Linear combination of atomic orbitals (LCAO) methods have not followed the same quick trend. One of the most important lines of development has been to obtain LCAO Hamiltonians from local-density approximation (LDA) calculations.[7] Other methods have tried to describe semiempirically LCAO Hamiltonians from the physical and chemical trends of different materials,[7] while in other works the basic LCAO Hamiltonian is obtained from the atomic properties of the ingredients forming the system.[9,10] Molecular dynamics calculations, based on LCAO Hamiltonians, have also been developed showing its applicability to complex situations.[11]

The point of view taken in this paper is that, using one of the methods commented on above, one can define the fundamental LCAO Hamiltonian, including many-body terms. In particular, this work can be considered as an extension of Ref. 9 where some of us have shown how a fundamental LCAO Hamiltonian can be obtained using the atomic wave functions of the species forming the system. Our aim is to show how the many-body contributions can be treated, within a LCAO formulation, using an extension of the LD approximation in a way similar to the procedure followed in standard density functional calculations. The advantage of this approach is that the formalism for analyzing many-body effects can be kept within the LCAO framework, by defining an exchange-correlation potential for each orbital without having to resort to conventional LD methods.

II. FORMALISM

In this section, we present the approach we propose for analyzing the many-body properties of LCAO Hamiltonians. First, the general formalism is presented; then, the exchange energy, as well as the extra-atomic and the intra-atomic correlation energies, are discussed and analyzed in successive steps.

A. General formalism

We follow Ref. 9 and take as our starting point the following Hamiltonian:

$$\hat{H} = \hat{H}^{\mathrm{oe}} + \hat{H}^{\mathrm{mb}}, \tag{1}$$

where $\hat{H}^{\mathrm{oe}}$ defines the one-electron contribution

$$\hat{H}^{\mathrm{oe}} = \sum_{i\sigma} E_i^{\sigma} \hat{n}_{i\sigma} + \sum_{\sigma,(i,j)} T_{ij}^{\sigma} (\hat{c}_{i\sigma}^{\dagger} \hat{c}_{j\sigma} + \hat{c}_{j\sigma}^{\dagger} \hat{c}_{i\sigma}), \tag{2}$$

and $\hat{H}^{\mathrm{mb}}$ the many-body terms

$$\hat{H}^{\mathrm{mb}} = \sum_i U_i \hat{n}_{i\uparrow} \hat{n}_{i\downarrow} + \frac{1}{2} \sum_{i,j\neq i,\sigma} (J_{ij} \hat{n}_{i\sigma} \hat{n}_{j\bar{\sigma}} + \tilde{J}_{ij} \hat{n}_{i\sigma} \hat{n}_{j\sigma}), \tag{3}$$

U_i, J_i, and $\tilde{J}_{ij}$ being the intrasite and intersite Coulomb interactions. The small differences found in Ref. 9 between J_{ij} and $\tilde{J}_{ij}$ due to the exchange integrals turn out to be small and will be neglected in the following discussion (take from now on $J_{ij} = \tilde{J}_{ij}$). In Eq. (2), E and T describe the different atomic levels and their hopping interactions, while their specific values can be obtained by using the wave functions of the independent atoms forming the system.[9]

Our interest here is to discuss how the many-body properties of Hamiltonian (1) can be analyzed using a LD scheme. The first point to notice regarding Hamiltonian (1) is that we can use the Hohenberg-Kohn[1] approach in the following way. First, define the interaction Hamiltonian

$$\hat{H}^{\rm int} = \sum_{i,\sigma} V_{i,\sigma}\hat{n}_{i\sigma}, \tag{4}$$

$V_{i,\sigma}$ being an external potential, and obtain the ground-state energy E_0 by the equation

$$\begin{aligned} E_0 &= \langle \phi_0 \mid \hat{H}^{\rm oe} + \hat{H}^{\rm mb} + \hat{H}^{\rm int} \mid \phi_0 \rangle \\ &= E^{\rm oe} + E^{\rm mb} + \sum_{i,\sigma} V_{i,\sigma} n_{i\sigma}, \end{aligned} \tag{5}$$

where $\mid \phi_0\rangle$ is the ground state of the total Hamiltonian, $\hat{H}+\hat{H}^{\rm int}$. Now, following the Hohenberg-Kohn approach, it is easy to prove that, under the usual condition of a nondegenerate ground state, there exists a biunivocal correspondence between the sets of parameters (V_1,V_2,...) and the ocupation numbers (n_1,n_2,...). This shows that the ground-state wave function $\mid \phi_0\rangle$, can be written as a function of the total Hamiltonian parameters, $E_i + V_i$, T_{ij}, U_i, and J_{ij}, or, alternatively, as a function of n_i, U_i, and J_{ij}, with $(E_i + V_i)$ replaced by the occupation numbers, n_i. It is obvious that, at this level, E_i only plays the role of a constant, changing the origin of the external perturbation. On the other hand, it is also convenient to realize that $\hat{H}^{\rm int}$ is just a mathematical tool that is used to prove that $\mid \phi_0\rangle$ can be written as a function of the sets of parameters, n_i, T_{ij}, U_i, and J_{ij} (this is also the case in the usual density functional approach for the perturbation $\int V(\bar{r})n(\bar{r})d\bar{r}$.

Then, $V_{i\sigma} + E_{i\sigma}$ appears as a unique function of $n_{i\sigma}$ ($V_{i\sigma} + E_{i\sigma}$=$\mathrm{V}_{i\sigma}[n_{1\uparrow}, n_{1\downarrow}, n_{2\uparrow}, n_{2\downarrow}, ...]$), where the other sets of parameters T_{ij}, U_i, and J_{ij} are understated. Hence, the occupation numbers $n_{i\sigma}$ uniquely determine the Hamiltonian $\hat{H} + \hat{H}^{\rm int}$ and the ground-state properties of the system.

In general, E_0 can be written down as a function of the sets of numbers $n_{i\sigma}$ as follows:

$$E_0[n_{i\sigma}] = E^{\rm oe}[n_{i\sigma}] + E^{\rm mb}[n_{i\sigma}] + \sum_{i,\sigma} V_{i,\sigma} n_{i\sigma}, \tag{6}$$

where the dependence on the other parameters T_{ij}, U_i, and J_{ij}, defining the initial Hamiltonian should be understood.

At this point, it is convenient to comment that in the usual density functional approach, E_0 is a function of $n(\bar{r})$ and the parameters defining the operators $-\frac{\hbar^2}{2m}\nabla^2$ and $\frac{e^2}{|\bar{r}-\bar{r}'|}$; in our approach T_{ij}, U_i, and J_{ij} play the same role as $\hbar$, m, and e^2 do in the conventional density functional scheme.

The actual densities $n_{i\sigma}$ associated with Hamiltonian (1) can be obtained by minimizing $E_0[\mathrm{n}_{i\sigma}]$ with respect to $\mathrm{n}_{i\sigma}$. Obviously, the energy for Hamiltonian (1) is given by Eq. (6) taking $V_{i\sigma} = 0$.

We can take a step further, and use the Kohn-Sham approach.[1] This is equivalent to solving self-consistently the following Hamiltonian:

$$\hat{H}_{\rm eff} = \hat{H}^{\rm oe} + \sum_{i,\sigma} V_{i\sigma}^{\rm mb}\hat{n}_{i\sigma}, \tag{7}$$

where $V_{i\sigma}^{\rm mb} = \frac{\partial E^{\rm mb}[n_{i\sigma}]}{\partial n_{i\sigma}}$; here, the occupation numbers $n_{i\sigma}$ are obtained solving Hamiltonian (7) with this local many-body local potential $V_{i\sigma}^{\rm mb}$.

Following the standard procedure we write $E^{\rm mb} = E^H + E^{\rm XC}$, with E^H and $E^{\rm XC}$ being the Hartree and the exchange-correlation energies, respectively. Then

$$V_{i\sigma}^H = \frac{\partial E^H[n_{i\sigma}]}{\partial n_{i\sigma}}\ ,\ V_{i\sigma}^{\rm XC} = \frac{\partial E^{\rm XC}[n_{i\sigma}]}{\partial n_{i\sigma}}. \tag{8}$$

From Eq. (3) we find that the Hartree energy is given by

$$E^H[n_{i\sigma}] = \sum_i U_i n_{i\uparrow} n_{i\downarrow} + \frac{1}{2}\sum_{i,j\neq i,\sigma} J_{ij} n_{i\sigma}(n_{j\bar{\sigma}} + n_{j\sigma}), \tag{9}$$

so that

$$V_{i,\sigma}^H = U_i n_{i\bar{\sigma}} + \sum_{j\neq i} J_{ij}(n_{j\bar{\sigma}} + n_{j\sigma}). \tag{10}$$

B. Exchange energy

The exchange-correlation energy $E^{\rm XC}$ can be split into its exchange E^X and correlation E^C contributions. The exchange term yields

$$E^X = -\frac{1}{2}\sum_{i,j\neq i,\sigma} J_{ij} n_{ij}^{\sigma} n_{ji}^{\sigma}, \tag{11}$$

where $n_{ij}^{\sigma} \equiv \langle \psi_0 \mid \hat{c}_{i\sigma}^{\dagger}\hat{c}_{j\sigma} \mid \psi_0\rangle$ is related to the bond-order index, a quantity that can be calculated[9] from the one-electron properties of the system. Notice that in defining n_{ij}^{σ} we have introduced the wave function $\mid \psi_0\rangle$; this is the ground-state wave function of the one-electron Hamiltonian, $\hat{H}^{\rm oe} + \hat{H}^{\rm int}$, that yields the same occupation numbers $n_{i\sigma}$ as the total Hamiltonian. Equation (11) is obtained from the term $J_{ij}\hat{n}_{i\sigma}\hat{n}_{j\sigma}$, by associating creation and annihilation operators belonging to $\hat{n}_{i\sigma}$ and $\hat{n}_{j\sigma}$, respectively.

In order to find the $n_{i\sigma}$ dependence of $E^X[n_{i\sigma}]$, it is convenient to use the following sum rule:[9] $\sum_j n_{ij}^{\sigma} n_{ji}^{\sigma} = n_{i\sigma}$. If one writes

$$n_{ij}^{\sigma} n_{ji}^{\sigma} = n_{i\sigma} g_{\sigma}(i,j), \tag{12}$$

the application of the sum rule yields

$$\sum_j g_{\sigma}(i,j) = 1, \tag{13}$$

with $g_{\sigma}(i,j)$ defining the pair correlation function associated with the exchange hole. Equation (12) allows us to write the exchange energy E^X as follows:

$$E^X = -\frac{1}{2}\sum_{i,j\neq i,\sigma} J_{ij} g_{\sigma}(i,j) n_{i\sigma}. \tag{14}$$

Thus, Eq. (14) states that E^X is associated with the interaction between an electron state, having occupancy $n_{i\sigma}$, and its exchange hole, measured by $g_{\sigma}(i,j)$.

To proceed further, it is convenient to approximate

provisionally Eq. (14) by assuming that the exchange hole is localized in the i-site nearest neighbors (NN). Within this approximation, the exchange energy is given by

$$E^X = -\frac{1}{2}\sum_{i,\sigma} J_i n_{i\sigma}(1-n_{i\sigma}), \tag{15}$$

where J_i is the Coulomb interaction between an electron in the $i\sigma$ orbital and another electron in its NN. Notice that from Eq. (13) we get $\sum_{j\neq i} g_\sigma(i,j) = 1 - n_{i\sigma}$, since $g_\sigma(i,i) = n_{i\sigma}$. Equation (15) yields the interaction between the $n_{i\sigma}$ charge and the hole, $(1-n_{i\sigma})$, localized in the NN: the extra $n_{i\sigma}$ hole needed for a total exchange hole of one is associated with the self-interaction correction that is automatically included in our formalism.

A more general case can be analyzed by considering different lattice structures (fcc or sc) having an s orbital per site and NN interaction. In these cases we obtain E^X by using Eq. (11) and calculating n_{ij}^σ from the one-electron Green function $G_{ij}^\sigma(\omega)$ of the system. Notice that for the simple cases considered here, the Hartree-Fock solution is the Slater determinant formed with the occupied one-electron states, $\sum_i e^{i\bar{k}\bar{R}_i}|s_i\rangle$, where $\bar{k}$ is the electron momentum and $|s_i\rangle$ the s orbital for the $\bar{R}_i$ site. We have written E^X as follows:

$$E^X = -\frac{1}{2}\sum_{i,\sigma} \alpha(n_{i\sigma}) J_i n_{i\sigma}(1-n_{i\sigma}), \tag{16}$$

where αJ_i is the effective interaction between charges $n_{i\sigma}$ and $-(1-n_{i\sigma})$.

For the different structures we have considered, $n_{i\sigma}$ is the site independent $i\sigma$ occupancy defined by the crystal Fermi energy. Our calculation yields $\alpha(\mathrm{n})$ as a function of the site occupancy. Figure 1 shows $\alpha(\mathrm{n})$ for the two chosen structures. Within the range $0.15 \leq n \leq 0.85$, $\alpha(\mathrm{n})$ is almost constant, varying smoothly around 0.75. This suggests that Eq. (15) can be generalized for an inhomogenous system (if $0.15 \leq n_{i\sigma} \leq 0.85$) to the form

$$E^X = \sum_{i\sigma} E_{i\sigma}^X = -\frac{1}{2}\sum_{i,\sigma} J_i \alpha_i n_{i\sigma}(1-n_{i\sigma}), \tag{17}$$

α_i being a constant that can be determined for each particular site using the one-electron properties of the system and Eq. (11).

On the other hand, the limit $n_{i\sigma} \to 0$ ($n_{i\sigma} \leq 0.1$), for the lattice structures analyzed above, makes contact between our approach and the usual LDA method. Notice that in this limit, electrons only fill a small pocket of states around $\bar{k} = 0$; then, the relevant filled states have the typical parabolic dispersion relation as in the free electron case. As Fig. 1 shows, for $n \to 0$, $\alpha(\mathrm{n})$ goes like $\mathrm{n}^{\frac{1}{3}}$, Eq. (13) yielding the $\mathrm{n}^{\frac{4}{3}}$-typical behavior of the exchange energy.

In the two examples just discussed, we have assumed to have a single orbital per site. More general cases correspond to having several orbitals per atom. For these cases, calculations performed for solid bulk crystal or surfaces (see Sec. III) show that the exchange hole for an orbital is basically localized outside its atom: then, Eq. (17) yields a good description of the exchange energy, if J_i is taken as the mean Coulomb interaction between the i orbital and the orbitals located in the nearest neighbor site; α_i is close to (but smaller than) one (if n_i is neither close to zero nor one), measuring how the exchange hole is spread around the neighboring atoms.

For most practical cases α_i can be taken constant; then, we can use Eq. (17) and the exchange potential $V_{i\sigma}^X$ takes the form

$$V_{i\sigma}^X = \frac{dE^X[n_{i\sigma}]}{dn_{i\sigma}} = \frac{dE_{i\sigma}^X[n_{i\sigma}]}{dn_{i\sigma}} = -\alpha_i J_i(\tfrac{1}{2} - n_{i\sigma}). \tag{18}$$

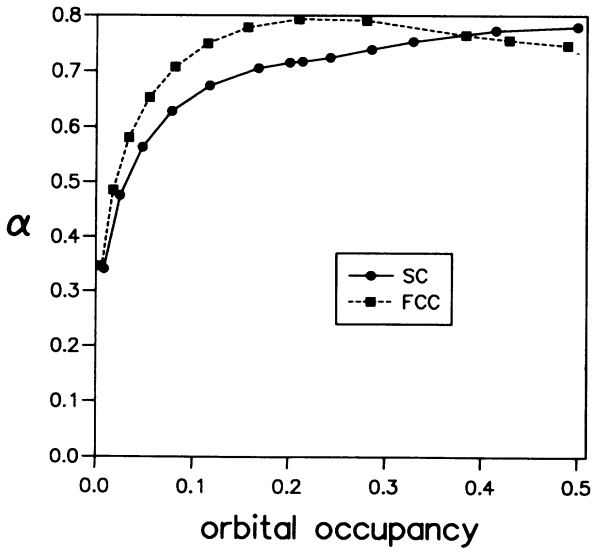

FIG. 1. $\alpha(n)$ as a function of the orbital occupancy for different lattice structures [see Eq. (16) and below]. In the range (0,1) $\alpha(n)$ is symmetric with respect to the point 0.5.

C. Extra-atomic correlation energy

We proceed now to discuss the correlation energy. In a first step, we shall concentrate our discussion in the extra-atomic effects; this means that the intra-atomic correlation energy will be provisionally neglected by assuming that the exchange-correlation hole is localized outside the orbital atom. We start our discussion for the extra-atomic correlation energy by considering the occupancy fluctuations for a given $i\sigma$ level. The occupancy $n_{i\sigma}$ represents the mean value for the different occupation numbers, 0 or 1. The mean Hartree energy associated with the mean electron charge $n_{i\sigma}$ and its screening hole $-n_{i\sigma}$ is given by $(-\frac{1}{2}I_i n_{i\sigma}^2)$, where I_i is the Coulomb interaction between an electron in the $i\sigma$ level and another electron distributed like the screening charge; the factor $\frac{1}{2}$ is due, as usual, to the adiabatic switching of the interaction and includes the electron kinetic energy associated with the screening effects.[13] Due to fluctuations, we have a probability $n_{i\sigma}$ of having the $i\sigma$ level filled,

and a probability $(1 - n_{i\sigma})$ of having it empty. As the Hartree energy associated with these two cases, weighted with their probabilities, is given by $-\frac{1}{2} I_i n_{i\sigma}$, we find that the energy associated with the occupancy fluctuations of the $i\sigma$ level is given by

$$E^f_{i\sigma} = -\tfrac{1}{2} I_i n_{i\sigma}(1 - n_{i\sigma}). \tag{19}$$

Now, as we are analyzing the extra-atomic correlation effects, we assume that the mean screening charge spreads out around the $i\sigma$ level like the exchange hole, localized outside the $i\sigma$ atom. This means that we take $I_i = \alpha_i J_i$, and $E^f_{i\sigma} = E^X_{i\sigma}$.

$E^f_{i\sigma}$ represents the static approximation to the Coulomb hole energy associated with the $i\sigma$ level. In a general formulation,[14] the exchange-correlation energy $E^{\rm XC}$ is given by the screened exchange interaction $E^{X,{\rm SC}}$ plus the Coulomb hole energy, $E^{\rm CH}$. It is well-known[13] that, for metallic densities, dynamical effects reduce the static value of the Coulomb hole energy by around 25%. Thus, we can write

$$E^{\rm CH} = \gamma E^f = \gamma \sum_{i\sigma} E^X_{i\sigma} \text{ with } \gamma = \tfrac{3}{4}. \tag{20}$$

The screened exchange interaction should be obtained by screening the $\alpha_i J_i$ factor in Eq. (17). We have calculated $E^{X,{\rm SC}}$ for $0.15 \leq n_{i\sigma} \leq 0.85$ by assuming, as mentioned above, that the screening charge spreads out around the $i\sigma$ level like its exchange hole. Our analysis yields that $E^{X,{\rm SC}}_{i\sigma} = \beta_i E^X_{i\sigma}$, with $0.70 \geq \beta_i \geq 0.30$ for $0.65 \leq \alpha_i \leq 0.95$ (β_i is found to depend almost linearly on α_i). Thus,

$$E^{X,{\rm SC}}_{i\sigma} = \beta_i E^X_{i\sigma} = -\frac{\beta_i}{2} \alpha_i J_i n_{i\sigma}(1 - n_{i\sigma}). \tag{21}$$

Equations (20) and (21) yield the following extra-atomic exchange-correlation energy per orbital:

$$E^{\rm XC}_{O,i\sigma} = -\frac{1}{2}(\gamma + \beta_i)\alpha_i J_i n_{i\sigma}(1 - n_{i\sigma}), \tag{22}$$

and shows that

$$E^C_{O,i\sigma} = (\beta_i + \gamma - 1) E^X_{i\sigma}, \tag{23}$$

for $0.15 \leq n_{i\sigma} \leq 0.85$.

Equation (22) yields the exchange-correlation energy as $\frac{1}{2}$ of the dynamically screened interaction between the charge n_i and its exchange-correlation hole,[13] $(1 - n_i)$. The extra n_i hole needed to complete the total hole[14] of one is still associated with the self-interaction correction. Notice that for $0.15 \leq n_{i\sigma} \leq 0.85$, $(\gamma + \beta_i)\alpha_i$ is close to one: this implies that the exchange-correlation hole is practically localized in the NN. Equations (8) and (22) yield our basic result for the extra-atomic exchange-correlation potential

$$V^{\rm XC}_{Oi\sigma} = -(\gamma + \beta_i)\alpha_i J_i (\tfrac{1}{2} - n_{i\sigma}), \tag{24}$$

with $(\gamma + \beta_i)\alpha_i \simeq 1$. From the different approximations made to obtain Eq. (22), we deduce that our ansatz for $E^{\rm XC}$ can have an inaccuracy not larger than 5%; this is still good enough since the energy $E^{\rm XC}$ per orbital is typically 1 eV (with $J_i \approx 6$ eV).

It is also convenient to make contact for the correlation energy with the LD approximation. To this end we consider the Wigner approximation for the correlation energy that offers an exact analysis of the low density limit. For the Wigner-correlation energy per electron we have the following equation:

$$E^C = -\frac{0.44}{1.0 + \left(\frac{4\rho}{3\pi}\right)^{-\frac{1}{3}}} \to_{\rho \to 0} -\left(\frac{4\rho}{3\pi}\right)^{\frac{1}{3}} 0.44 \text{ a.u.}, \tag{25}$$

ρ being the electron density. This equation should be compared with the exchange energy per electron (LDA), $E^X = -\frac{3}{4}(\frac{3\rho}{\pi})^{\frac{1}{3}}$ a.u.

This shows that

$$E^C = 0.959 E^X \text{ for } \rho \to 0. \tag{26}$$

We recover a very similar Eq. ($E^C = E^X$) from our approach by neglecting all the screening effects in the exchange interaction and the Coulomb hole energy, as should be done in the very low electron density limit. This suggests that $\beta \to 1$ for $n_{i\sigma} \to 0$, a result consistent with the values given above for β_i; a linear extrapolation of these values shows that $\beta_i = 1$ for $\alpha_i \simeq 0.4$. Also for electron densities much smaller than typical densities $\gamma \to 1$.

D. Intra-atomic correlation energy

Up to this point we have only considered extra-atomic correlation contributions to $E^{\rm XC}$. Intra-atomic effects are negligible for very electropositive atoms (typically, alkali atoms), but they can be very important for the very electronegative ones (extreme cases are O,F, etc.). Intra-atomic correlation effects are associated with having the exchange-correlation hole $(1 - n_{i\sigma})$ extended to the atom of the orbital. In the following discussion, we shall assume that all the orbitals inside the atom interact with each other with the same Coulomb interaction U (small differences between these interactions are not relevant to the discussion presented here). Then, it is convenient to rewrite the extra-atomic exchange-correlation energy, Eq. (22), as follows:

$$E^{\rm XC}_{O,i\sigma} = -\tfrac{1}{2} J_{0,i} n_{i\sigma}(1 - n_{i\sigma}), \tag{27}$$

where $J_{0,i}$ represents the effective interaction between the $n_{i\sigma}$ charge and its exchange-correlation hole $(1 - n_{i\sigma})$. Intra-atomic correlation effects appear when part of the total exchange-correlation hole is transferred to the same atom of the $i\sigma$ orbital. If a fraction, say $f (f < 1)$, of this hole is located in the atom, the intra-atomic correlation energy should be given by

$$E^C_{I,i\sigma} = -\frac{f}{2} U_i n_{i\sigma}(1 - n_{i\sigma}), \tag{28}$$

where U_i is the intrasite Coulomb interaction between orbitals, f being, in general, a function of U_i, T_{ij}, and

n_i. At the same time, the extra-atomic correlation energy should be reduced due to having only a fraction, $(1-f)(1-n_{i\sigma})$, of the hole outside the atom. Then, the total exchange-correlation energy is given by

$$\begin{aligned} E^{\mathrm{XC}}_{i\sigma} &= E^{\mathrm{XC}}_{O,i\sigma} + E^{C}_{I,i\sigma} \\ &= -\frac{1}{2}(1-f)J_{0,i}n_{i\sigma}(1-n_{i\sigma}) - \frac{f}{2}U_i n_{i\sigma}(1-n_{i\sigma}) \\ &= -\tfrac{1}{2}J_{0,i}n_{i\sigma}(1-n_{i\sigma}) - \frac{f}{2}(U_i - J_{0,i})n_{i\sigma}(1-n_{i\sigma}). \end{aligned} \tag{29}$$

This equation shows that intra-atomic correlation effects can be added to the extra-atomic exchange-correlation energy by considering an effective interaction $(U_i - J_{0,i})$ and the hole-fraction f that is localized inside the atom.

We have calculated this parameter f by considering different cluster models that try to simulate the conditions we are interested in. Figures 2 and 4 show the cases we have considered in order to obtain the correlation effects associated with atoms of different valency. All these cases have been solved exactly using the corresponding configurational space. Thus, for monovalent atoms we have used the clusters shown in Fig. 2. The first case [Fig. 2(a)] corresponds to an atom chemisorbed on a metal surface simulated by three atoms, with the cluster having four electrons; its Hamiltonian is given by

$$\begin{aligned} \hat{H}^c = &\sum_{i=1,3\sigma} \epsilon_M \hat{n}_{i\sigma} + \sum_{\sigma} t(\hat{c}^{\dagger}_{1\sigma}\hat{c}_{2\sigma} + \hat{c}^{\dagger}_{2\sigma}\hat{c}_{3\sigma} + \text{c.c.}) \\ &+ \sum_{\sigma} \epsilon_0 \hat{n}_{0\sigma} + \sum_{\sigma} T(\hat{c}^{\dagger}_{0\sigma}\hat{c}_{3\sigma} + \hat{c}^{\dagger}_{3\sigma}\hat{c}_{0\sigma}) \\ &+ U_{\mathrm{eff}}\hat{n}_{0\uparrow}\hat{n}_{0\downarrow}. \end{aligned} \tag{30}$$

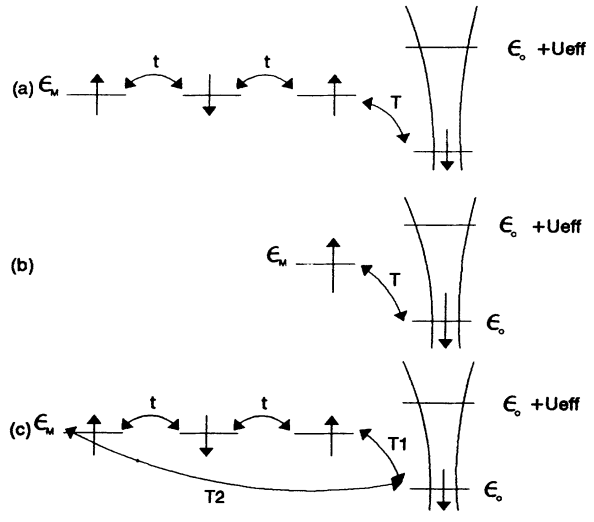

FIG. 2. Shows different clusters used to calculate the intra-atomic correlation energy for a monovalent atom. Clusters (a), (b), and (c) have 4, 2, and 4 electrons, respectively. The total spin of each cluster is chosen to be zero.

The case shown in Fig. 2(b) corresponds to a similar condition, but the metal is simulated only by an atom. The case shown in Fig. 2(c) tries to simulate a monovalent atom inside a metal. In all these cases, correlation effects are localized in a single atom. By solving the model Hamiltonian of Eq. (30), we expect to obtain information about the intra-atomic correlation energy and the correlation hole that is localized in the same atom.

In our calculation,[15] ϵ_0 the adatom level is changed and the total energy E_0 and the level occupancy $n_{0\sigma}$ are calculated for the ground state. Then, the one-electron energy of Hamiltonian (30) is obtained by solving independently the one-electron Hamiltonian

$$\begin{aligned} \hat{H}^c = &\sum_{i=1,3\sigma} \epsilon_M \hat{n}_{i\sigma} + \sum_{\sigma} t(\hat{c}^{\dagger}_{1\sigma}\hat{c}_{2\sigma} + \hat{c}^{\dagger}_{2\sigma}\hat{c}_{3\sigma} + \text{c.c.}) \\ &+ \sum_{\sigma} V_0 \hat{n}_{0\sigma} + \sum_{\sigma} T(\hat{c}^{\dagger}_{0\sigma}\hat{c}_{3\sigma} + \hat{c}^{\dagger}_{3\sigma}\hat{c}_{0\sigma}), \end{aligned} \tag{31}$$

with V_0 adjusted to give the same charge $n_{0\sigma}$ as the one obtained for Hamiltonian (30). The one-electron kinetic and potential energies for Hamiltonian (30) are calculated using the ground-state wave function of Hamiltonian (31); the correlation energy is given by the difference between the total energy E_0 and the one-electron energies. Obviously, the other cases shown in Fig. 2 have been solved following the same steps.

Let us, first of all, discuss the results obtained for the cluster shown in Fig. 2(a). The first point to comment is that f [Eq. (29)] has been found to depend on $n_{0\sigma}$ and $\frac{U_{\mathrm{eff}}}{T}$ as shown in Fig. 3(a), with a negligible dependence on t, for t not much larger than T. For values of $\frac{U_{\mathrm{eff}}}{T}$ smaller than 8, f is practically proportional to $\frac{U_{\mathrm{eff}}}{T}$, its behavior as a function of $n_{0\sigma}$ being in this region basically the same, except for a constant, for all values of $\frac{U_{\mathrm{eff}}}{T}$. This is the region of major interest as $\frac{U_{\mathrm{eff}}}{T} > 8$ corresponds to a physical condition of very small bonding. It is also convenient to rewrite the intra-atomic correlation energy in the following way:

$$\begin{aligned} E^{C}_{I,i\sigma} &= -\frac{f}{2}U_{\mathrm{eff}}n_{i\sigma}(1-n_{i\sigma}) \\ &= -\frac{1}{2}\frac{U_{\mathrm{eff}}}{4}\lambda\left(\frac{U_{\mathrm{eff}}}{T}\right)\epsilon^{C}_{I}\left(n_{0\sigma}, \frac{U_{\mathrm{eff}}}{T}\right), \end{aligned} \tag{32}$$

where the factor ϵ^C_I is normalized to one at $n_{0\sigma} = \frac{1}{2}$, and λ embodies all the dependence on $\left(\frac{U_{\mathrm{eff}}}{T}\right)$ at this point. Figure 3(b) shows ϵ^C_I as a function of $n_{0\sigma}$ for different values of $\frac{U_{\mathrm{eff}}}{T}$; for $\frac{U_{\mathrm{eff}}}{T} < 8$, the region of major interest ϵ^C_I changes very little, while for $\frac{U_{\mathrm{eff}}}{T} \to \infty$, ϵ^C_I is deformed developing a cusp around the point $n_0 = \frac{1}{2}$. Figure 3(c) shows λ as a function of $\frac{U_{\mathrm{eff}}}{T}$: notice the linear behavior up to around $\frac{U_{\mathrm{eff}}}{T} = 8$, and the saturation to 1 when $\frac{U_{\mathrm{eff}}}{T} \to \infty$. It is interesting to see that the intra-atomic correlation potential V^C_I,

$$V^{c}_{I} = \frac{dE^{C}}{dn_I} = -\lambda\frac{U_{\mathrm{eff}}}{8}\frac{d\epsilon^{C}_{I}}{dn_0} \tag{33}$$

goes to $\pm\frac{U_{\mathrm{eff}}}{2}$ around $n_0 = \frac{1}{2}$, for $\frac{U_{\mathrm{eff}}}{T} \to \infty$. This re-

sult is related to the fact that for a very small coupling between the atom and the metal, if the Fermi energy is located between the atomic ionization and affinity levels, the correlation potential tends to align the effective atomic level and the Fermi energy; the reason is that that solution yields the $\frac{1}{2}$ occupancy of the atomic level. It should also be noticed in this regard that, in this limit ($\frac{U_{\rm eff}}{T} \to \infty$), the intra-atomic correlation energy per spin is $\frac{U_{\rm eff}}{8}$ as it should be. It should be noticed that the limit $\frac{U_{\rm eff}}{T} \to \infty$ does not prevent having $n_{0\sigma}$ spanning the full range (0,1): the reason is that V_0 can always be chosen to fix the $n_{0\sigma}$ value. For instance, for $V_0 = -\frac{U_{\rm eff}}{2}$ we always get $n_{0\sigma} = \frac{1}{2}$, and for $V_0 \ll \frac{U_{\rm eff}}{2}$, $n_{0\sigma}$ approaches one.

Once we have discussed the results found for the cluster of Fig. 2(a), we shall comment on the ones found for the other clusters of Figs. 2(b) and 2(c). The main point to notice is that these two cases yield results similar to the previous one; in particular the cases of Figs. 2(a) and 2(b) are almost completely equivalent: this suggests that the small cluster of Fig. 2(b) embodies the main properties of the larger cluster of Fig. 2(a) and, probably, of similar clusters with more atoms in the metal chain. Regarding the cluster shown in Fig. 2(c), its correlation properties are found to be equivalent to the ones of the cluster of Fig. 2(a) for the same effective couplings between the atom and the metal; in this regard, the effective coupling of the Fig. 2(c) cluster is found to be $T_{\rm eff} = (T_1^2 + T_2^2)^{\frac{1}{2}}$ as corresponds to the atom coupled to two metal atoms with the hoppings, T_1 and T_2.

The case of divalent atoms interacting with metals has been analyzed using the simple case of Fig. 4(a); this is equivalent to the Fig. 2(b) cluster that embodies the main properties of a monovalent atom coupled to a metal. Notice that in Fig. 4(a), the two metal levels are decoupled to each other: this decoupling allows us to prevent exchange effects to appear inside the atom, as is the usual case in crystals. Correlation effects are introduced by means of the Coulomb interaction acting between different levels: in our model all these interactions are set equal to $U_{\rm eff}(U_1 = U_2 = J_{12} = U_{\rm eff})$. The solution for the cluster of Fig. 4(a) has also been obtained using the method explained above for the clusters of Fig. 2(a).

Figures 5(a) and 5(b) show the intra-atomic correlation energy E_I^C as a function of $n_{1\sigma}$ and $n_{2\sigma}$ for $\frac{U_{\rm eff}}{T} = 3$ and 6. We have found that E_I^C can be written, in the range $0.1 < n_{1\sigma}, n_{2\sigma} < 0.9$ with a very good accuracy as follows:

$$E_I^C = \sum_{i\sigma} E_{I,i\sigma}^C = -\frac{U_{\rm eff}}{8}\lambda\left(\frac{U_{\rm eff}}{T}\right)\sum_{i\sigma}\epsilon_I^C\left(n_{i\sigma};\frac{U_{\rm eff}}{T}\right)$$
$$\approx -\frac{U_{\rm eff}}{8}\lambda\left(\frac{U_{\rm eff}}{T}\right)\sum_{i\sigma}\epsilon_I^C(n_{i\sigma}), \qquad (34)$$

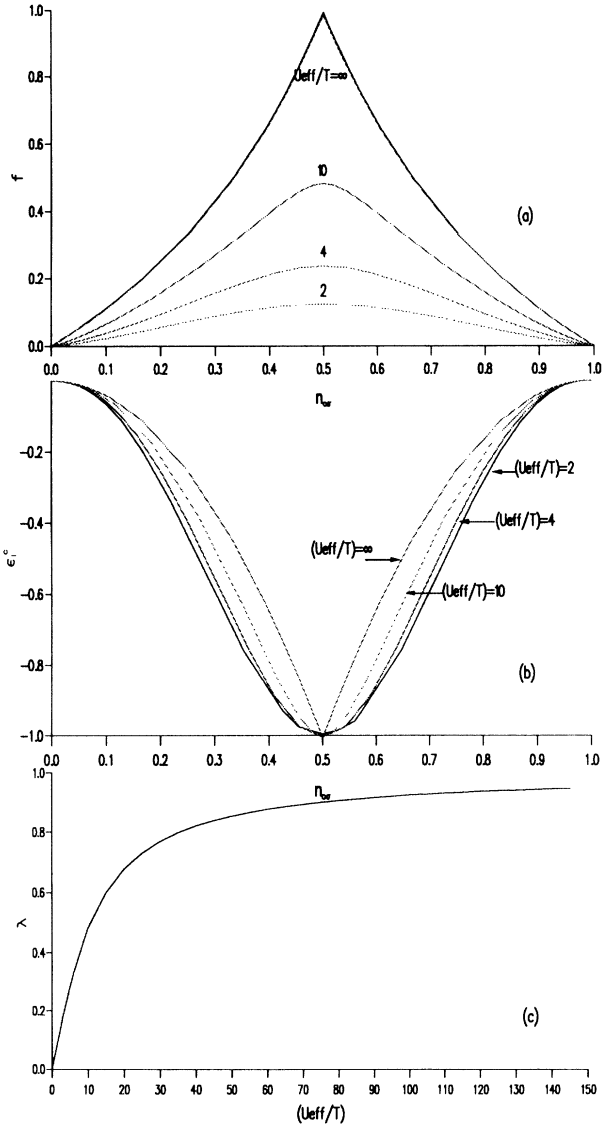

FIG. 3. (a) $f(n_{0\sigma}, \frac{U_{\rm eff}}{T})$, see Eq. (28), is shown as a function of $n_{0\sigma}$ for different $\frac{U_{\rm eff}}{T}$ values for the cluster of Fig. 2(a). (b) The same for $\epsilon_I^C(n_{0\sigma}, \frac{U_{\rm eff}}{T})$, see Eq. (32). (c) $\lambda(\frac{U_{\rm eff}}{T})$, see Eq. (28), is shown as a function of $\frac{U_{\rm eff}}{T}$ for the cluster of Fig. 2(a).

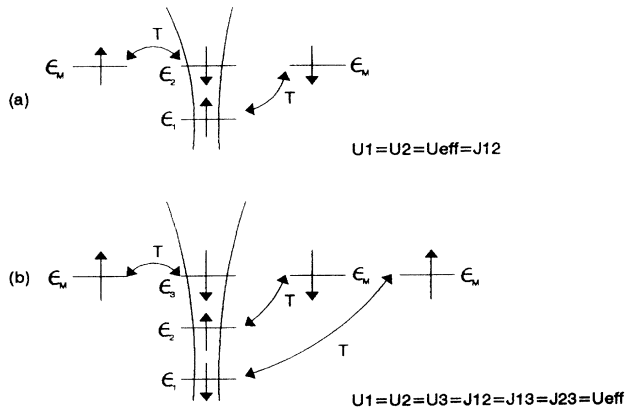

FIG. 4. Shows different clusters used to calculate the intra-atomic correlation energy for (a) a divalent atom and (b) a trivalent atom.

where $\epsilon_I^C(n_{i\sigma})$ is the function shown in Fig. 6(a), practically independent of $\frac{U_{\text{eff}}}{T}$ (if $\frac{U_{\text{eff}}}{T} < 6$), that embodies all the dependence on the orbital occupancies, $n_{i\sigma}$. Equation (34) yields the intra-atomic correlation function as a sum of the contributions coming from each independent atomic orbital. We should stress that Eq. (34) is found to be valid only if the charges $n_{i\sigma}$ are not too close to either 0 or 1. In particular, if, say, $n_{2\sigma} = 0$, the correlation energy coincides with the case discussed for a monovalent atom, with ϵ_I^C given above in Fig. 3(c). Notice that for the divalent case, the curve shown in Fig. 6(a) is a little broader than the ones shown in Fig. 3(b): this is the result of a larger intra-atomic correlation energy associated with the increasing valency of the atom.

Figure 6(b) shows $\lambda(\frac{U_{\text{eff}}}{T})$, the function that embodies all the dependence on $\frac{U_{\text{eff}}}{T}$. Compare this curve with the one shown in Fig. 3(c) to see the important effects introduced by the larger atomic valency. As the values $\frac{U_{\text{eff}}}{T} < 6$ cover most of the cases of physical interest, the results of Fig. 6 are sufficient to allow us to analyze the intra-atomic correlation effects for a divalent atom using the almost "universal" curve $\epsilon_I^C(n)$, and the λ values of Fig. 6(b). Let us mention that as $\frac{U_{\text{eff}}}{T}$ increases, the $\epsilon_I^C(n_\sigma)$ curves get narrower as discussed for the monovalent case.

Finally, we consider a trivalent atom interacting with a metal. This has been analyzed using the cluster drawn in Fig. 4(b), with the three atomic levels interacting with three independent levels that simulate a metal. The results we have found for this case can also be embodied in the equation (for $\frac{U_{\text{eff}}}{T} < 6$),

$$E_I^C = \sum_{i\sigma} E_{I,i\sigma}^C = -\frac{U_{\text{eff}}}{8}\lambda\left(\frac{U_{\text{eff}}}{T}\right)\sum_{i\sigma}\epsilon_I^C\left(n_{i\sigma};\frac{U_{\text{eff}}}{T}\right)$$

$$\approx -\frac{U_{\text{eff}}}{8}\lambda\left(\frac{U_{\text{eff}}}{T}\right)\sum_{i\sigma}\epsilon_I^C(n_{i\sigma}), \tag{35}$$

where, as in the divalent case, E_I^C is written as the sum of the independent orbital contributions. $\epsilon_I^C(n)$ is shown in Fig. 6(b); here, we see that ϵ_I^C can be very well approximated by $4n_{i\sigma}(1 - n_{i\sigma})$, in the range $0.1 < n_{i\sigma} < 0.9$.

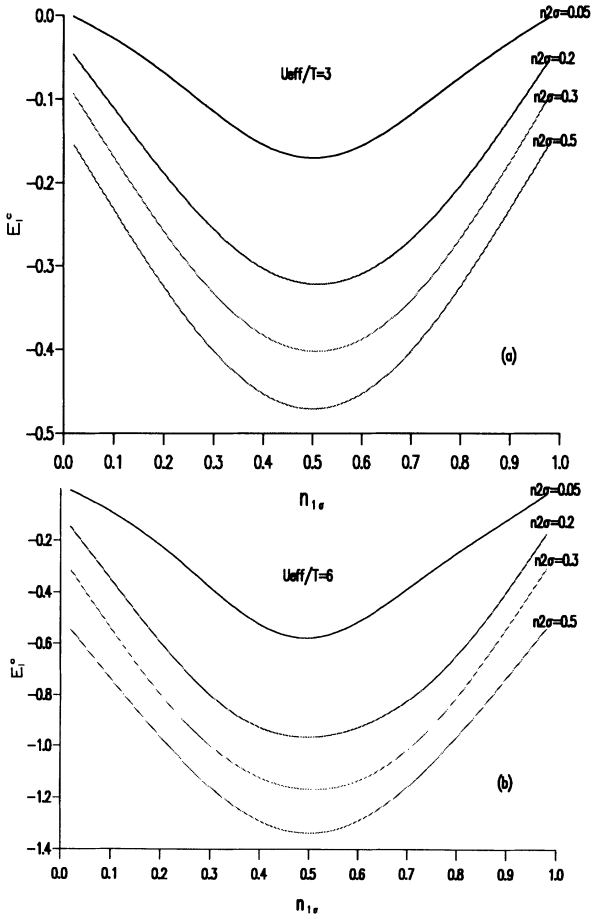

FIG. 5. The intra-atomic correlation energy E_I^C for the divalent model of Fig. 4 is shown as a function of $n_{1\sigma}$ for different values of $n_{2\sigma}$ (0.05, 0.2, 0.3, and 0.5). Curves $n_{2\sigma}$ are symmetric with respect to $n_{1\sigma} = 0.5$ of $(1 - n_{2\sigma})$ curves. We take T=1. (a) Here $\frac{U_{\text{eff}}}{T} = 3$. (b) $\frac{U_{\text{eff}}}{T} = 6$.

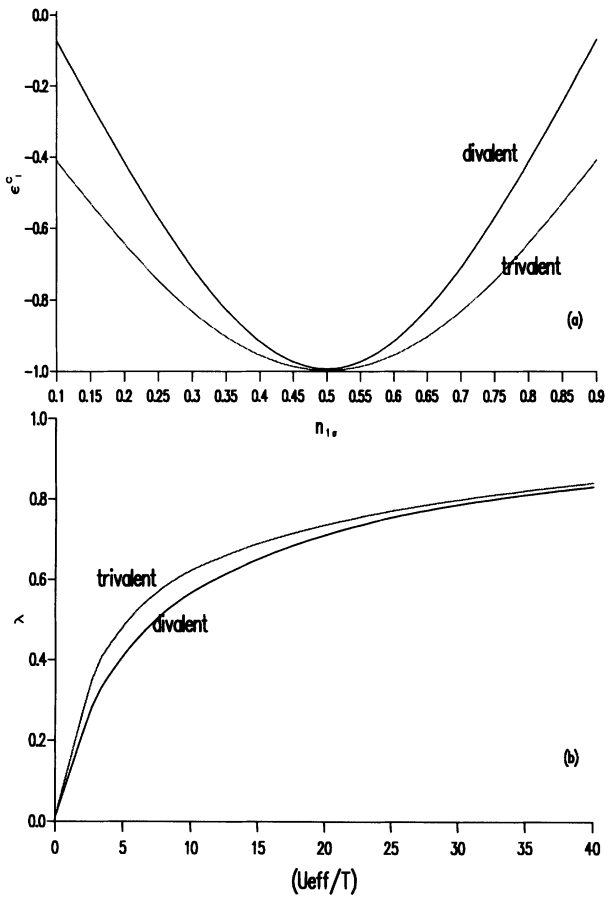

FIG. 6. (a)$\epsilon_I^C(n_\sigma)$ for the divalent (full line) and trivalent (dashed line) models of Fig. 4 is shown as a function of n_σ. (b) $\lambda\left(\frac{U_{\text{eff}}}{T}\right)$ for the divalent (full line), and the trivalent (dashed line) models of Fig. 4 is shown as a function of $\frac{U_{\text{eff}}}{T}$.

This shows that

$$E_I^C = -\sum_{i\sigma} \frac{U_{\text{eff}}}{2} \lambda \left(\frac{U_{\text{eff}}}{T} \right) n_{i\sigma}(1 - n_{i\sigma}), \tag{36}$$

with $\lambda \left(\frac{U_{\text{eff}}}{T} \right)$ as given in Fig. 6(b).

The discussion presented here for intra-atomic correlation effects has focused on different atoms interacting with a metal. If the matrix with which the atom is interacting is a semiconductor, things are slightly different because the semiconductor energy gap tends to increase the intra-atomic correlation energy. This has been analyzed by means of the cluster shown in Fig. 7(a), for a monovalent atom. The correlation energy per spin has also been calculated as in previous cases. Using the same equation as defined above

$$E_{I,i\sigma}^C = -\frac{U_{\text{eff}}}{8} \lambda \left(\frac{U_{\text{eff}}}{T}, \frac{t}{U_{\text{eff}}} \right) \epsilon_I^C(n_{1\sigma}), \tag{37}$$

we have determined λ for different $\frac{U_{\text{eff}}}{T}$ and $\frac{t}{U_{\text{eff}}}$ parameters. For $\frac{t}{U_{\text{eff}}} \to 0$ we recover the case already discussed [see Fig. 3(c)]. For increasing values of $\frac{t}{U_{\text{eff}}}$, $E_{I,i\sigma}^C$ increases as shown in Fig. 7(b), where λ is given as a function of $\frac{U_{\text{eff}}}{T}$ for different $\frac{t}{U_{\text{eff}}}$ values. Typically, $\frac{t}{U_{\text{eff}}} < \frac{1}{3}$, and Fig. 7(b) shows a slight increase (less than 20%) in the correlation energy due to the semiconductor gap effects. Let us also mention that $\epsilon_I^C(n_{i\sigma})$ in Eq. (37) practically coincides with the curve found above for the monovalent case.

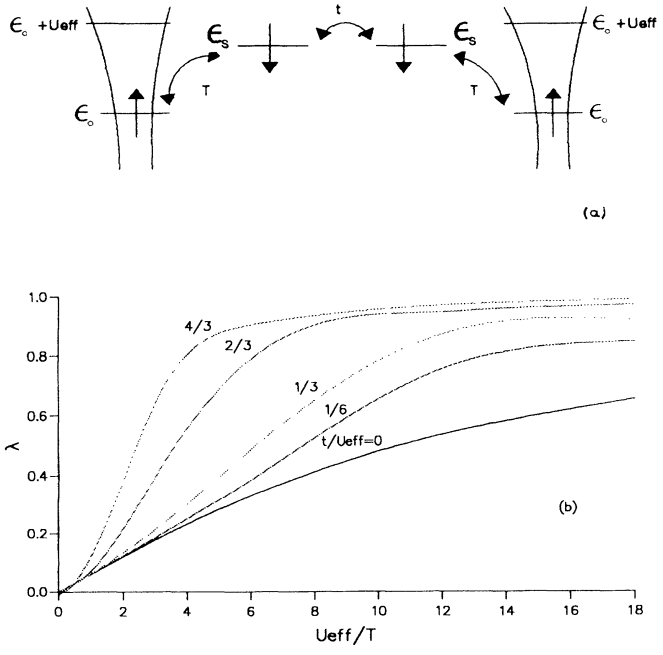

FIG. 7. (a) Model used to calculate the semiconductor gap effects in the intra-atomic correlation energy. Here $2t$ yields the semiconductor gap. (b) $\lambda \left(\frac{U_{\text{eff}}}{T}, \frac{t}{U_{\text{eff}}} \right)$ is shown as a function of $\frac{U_{\text{eff}}}{T}$ for different $\frac{t}{U_{\text{eff}}}$ values.

Summarizing this section, the total exchange-correlation energy for a given level can be written as follows:

$$\begin{aligned} E_{i\sigma}^{\text{XC}} &= -\tfrac{1}{2} J_{0,i} n_{i\sigma}(1 - n_{i\sigma}) - \tfrac{f}{2}(U_i - J_{0,i}) n_{i\sigma}(1 - n_{i\sigma}) \\ &= -\tfrac{1}{2} J_{0,i} n_{i\sigma}(1 - n_{i\sigma}) - \frac{(U_i - J_{0,i})}{8} \lambda \epsilon_I^C(n_{i\sigma}), \end{aligned} \tag{38}$$

with two terms yielding the contributions coming from the extra-atomic and intra-atomic effects. For very electropositive atoms, intra-atomic effects are negligible and we only get the extra-atomic contribution, $-\frac{1}{2} J_{0,i} n_{i\sigma}(1 - n_{i\sigma})$.

In more general cases, the intra-atomic correlation energy, $-\frac{f}{2}(U_i - J_{0,i}) n_{i\sigma}(1 - n_{i\sigma})$ is important. It should also be kept in mind that there is a particular balance between intra-atomic and extra-atomic effects, as the limit $\frac{U_i}{T_i} \to \infty$ shows. Here $f \to 1$ and the total exchange-correlation energy reads $-\frac{U_i}{2} n_{i\sigma}(1 - n_{i\sigma})$; this only means that in this limit the exchange-correlation hole is completely localized inside the atom.

III. RESULTS

As an application of the previous formalism we have analyzed two cases, the adsorption of Na on Al(100), a case where the intra-atomic correlation effects are negligible, and the adsorption of H on the GaAs(110) surface, a case for which those intra-atomic effects get relevant. In this last case, we shall also discuss how H interacts with the semiconductor surface at long distances, when the extra-atomic many-body effects are negligible. The Na case has been analyzed by using the LCAO Hamiltonian defined above, with the parameters calculated as explained in Ref. 9.

In our approach, we have considered different Na coverages $\theta = 1$, $\frac{1}{2}$, and $\frac{1}{4}$ ($\theta = 1$ is a monolayer, with a Na atom per Al unit cell), and have introduced many-body effects as explained above by taking $\beta_i = 0.7$, as the exchange energy is found to be given by Eq. (17) with $\alpha_i = 0.65$. In our treatment, the metal surface is described by using a semiempirical approach,[16] and the fully LCAO-consistent method is applied to obtaining the interaction between the Na layer and the metal surface. The aim of this calculation is to analyze the charge transfer between the Na atoms and the metal. Figure 8 shows the chemisorption energy per Na atom as a function of the distance between the alkali layer and the last metal layer (in the calculations presented here, the Na atoms move along the surface fourfold position). Our results show a strong evolution of the chemisorption energy as a function of the coverage; this is mainly due to the repulsive interaction between the alkali atoms for large coverages and is in good agreement with LDA calculations.[17] We should mention that the correct treatment of the extra-atomic exchange-correlation energy is crucial for obtaining a positive binding energy: in our calculations E^{XC} per adsorbed atom is 2.34, 2.38, and 2.88 eV for $\theta = 1$, $\frac{1}{2}$, and $\frac{1}{4}$, respectively.

We should also mention that our calculations yield the

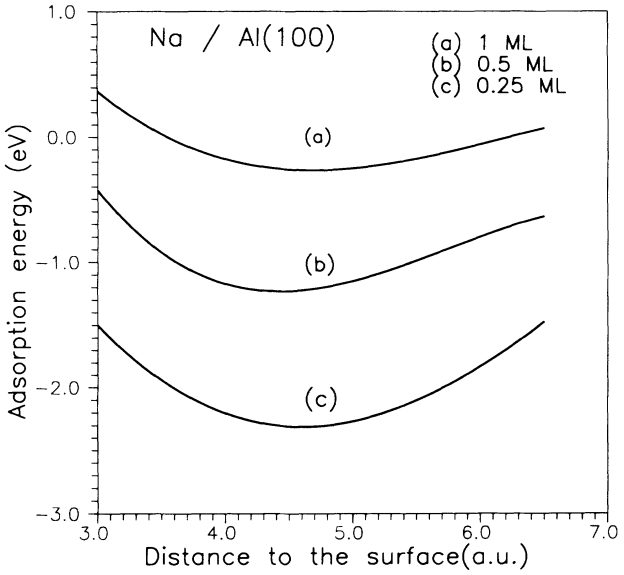

FIG. 8. Chemisorption energy per adsorbed atom for Na on Al(100) as a function of the distance between a Na atom and the last metal layer. Different curves correspond to different coverages, $\theta = 1$, $\theta = 0.5$, and $\theta = 0.25$.

following electronic charge per Na atom: 0.97, 0.82, and 0.7 electrons for $\theta = 1$, $\frac{1}{2}$, and $\frac{1}{4}$, respectively. This shows an important evolution from a very covalent regime ($\theta = 1$) to an intermediate case ($\theta = \frac{1}{4}$) where Na has 0.7 electrons. It is important to notice that we do not recover the pure ionic limit, with the alkali atom completely ionized, in the low coverage regime: this is also in agreement with the results of Refs. 17 and 18. Our self-consistent approach, with the treatment of the exchange and correlation effects as discussed above, offers a very convenient way of analyzing how the electron charge is transferred between the adsorbate and the metal; the problem associated with the usual LDA method is related to the difficulty in obtaining the ion charge from the total charge density.

We have also applied the previous formalism to calculate the interaction between a H atom and the GaAs(110) surface. The semiconductor surface is described using Vogl *et al.*'s parameters,[19] and the method discussed here is applied to the calculation of the interaction between H and the semiconductor. The exchange-correlation potential introduced in this paper allows us to obtain in detail the H-chemisorption energy not only for H-semiconductor distances around the energy minimum, but at large distances, too. Notice that at these large distances, the intra-atomic correlation energy should cancel very accurately the intra-atomic Coulomb interaction energy appearing between electrons having opposite spins: the correlation potential introduced in Sec. II yields this cancellation with good accuracy.

In this paper, we present results for the chemisorption of half a monolayer of H deposited on the As site (a monolayer corresponds to two atoms per semiconductor unit cell). It is well known that H chemisorbs on both As and Ga atoms with similar bond strengths,[20] then, we can expect the H atoms to be equally deposited on the two semiconductor dangling bonds. Our interest in analyzing the case of a H monolayer deposited on the As dangling bonds is addressed to understanding how the As-H bond is formed, and how the As-like dangling bonds are modified by the H deposition. In particular, the H-H distances inside the monolayer is large enough to practically decouple the H-H interaction. Thus, the H semiconductor interaction is very similar to the one between independent H atoms and the As dangling bonds.

Figure 9 shows the chemisorption energy per H atom as a function of the H-semiconductor distance. In the same figure, we also show the different contributions to the chemisorption energy: the repulsive energy is due to the overlap between the electron charge clouds of H and the semiconductor; the hybridization energy is associated with the hopping integrals T and also includes the Coulomb interaction between charges, except for the intrasite Coulomb interaction $\frac{U}{4}$ that is shown independently; finally, the exchange-correlation energy is also shown in Fig. 9.

From this figure, we deduce that the H-As coupling starts to appear for distances smaller than 2.6 Å, while the energy minimum is obtained for $d = 1.9$ Å. For $d >$ 2.6 Å, the H-As interaction is practically zero, with a very good cancellation between all the different terms contributing to the total energy. For distances larger than 3.2 Å, the exchange-correlation energy is cancelling out the intra-atomic repulsive energy $\frac{U}{4}$ and all the other interactions start to be negligible.

In order to show how the H-As bond is formed, we

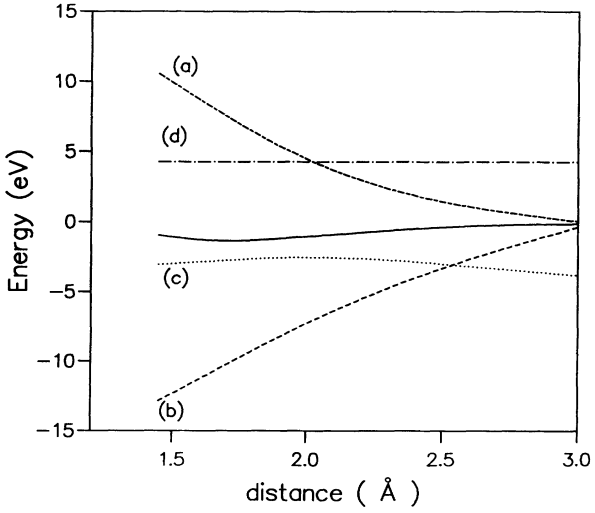

FIG. 9. Chemisorption energy (full line) per adsorbed atom for H on GaAs(110) as a function of the H-semiconductor distance. This energy is split into its different contributions: (a) repulsive energy, (b) hybridization energy, (c) exchange-correlation energy, and (d) the intrasite Coulomb interaction for H, $\frac{U}{4}$.

show in Fig. 10 how the local density of states on the H and the last semiconductor layer evolve as a function of the H-semiconductor distance. For $d = 3.4$ Å, Fig. 10(a) shows a H-prominent peak associated with the atomic level; the semiconductor layer shows the two peaks associated with the As-like and the Ga-like surface states. For $d = 2.6$ Å, when the H and As starts to form the bond, we find that the H peak has been shifted upwards in energy due to the As interaction, while the As-like peak has also been displaced downward due to the same effect. Eventually, Fig. 10(c) shows the case $d = 1.9$ Å, for the chemisorption energy minimum: in this case the strong H-As interaction has evolved to its full strength, and the H and As peaks of the decoupled system [see Fig. 10(a)] have been completely removed from the semiconductor gap. We only find the surface band associated with the Ga-like dangling bonds.

Similar results have been obtained for Ga. For the Ga-H bond we find that the Ga-like initial states located around the semiconductor gap are also removed from this region by the Ga-H interaction. Accordingly, a full H monolayer is found to passivate the semiconductor surface. Finally, let us mention that for this full monolayer, the chemisorption energy per adsorbed atom is obtained to be ≈ 2.5 eV, this result showing a strong interaction between the hydrogens adsorbed on the Ga and As dangling bonds.

IV. CONCLUSIONS

In conclusion, we have presented a self-consistent LD approach for analyzing LCAO Hamiltonians. The method is always kept at the level of the initial atomic orbitals basis, the exchange-correlation energy being described as a function of the orbital occupancies. Equation (38) defines the many-body energy as the contribution of two terms: one is related to the extra-atomic exchange-correlation effects, the second one to intra-atomic correlation processes. Both energies are described in the pa-

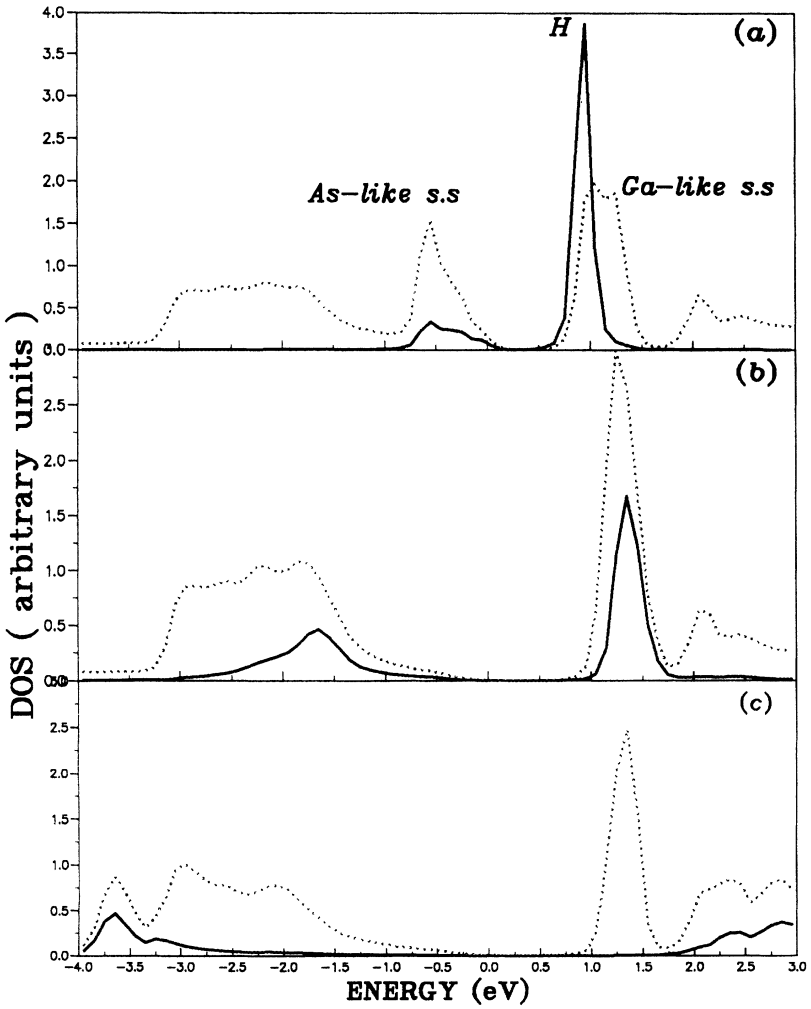

FIG. 10. Local density of states on H (full line) and the last semiconductor layer (dotted line) for different H-semiconductor distances: (a) $d = 3.4$ Å; (b) $d = 2.6$ Å; (c) $d = 1.9$ Å. s.s. means surface state.

per, and the parameters defining these contributions are calculated using simple, but reasonable, approximations.

The scheme derived in this paper has been applied to two different systems: in the first one, only extra-atomic many-body effects are important. This is the case of an alkali atom, Na, on Al(100). Our results offer a convenient way to analyze the problem of the charge transfer between the alkali atom and a metal. In the second system, we have analyzed H chemisorbed on GaAs(110) and have described how the bond between the H and As is formed. Our procedure has been applied to the calculation of the H-As chemisorption energy for long distances, too, a limit where intra-atomic correlation effects are very important. Our results for the H case suggests that H is strongly bonded to the different semiconductor dangling-bonds, and that a H monolayer would tend to passivate the surface leaving no density of states in the semiconductor energy gap.

The good results obtained for the different systems analyzed in this paper give strong support to the method introduced here.

ACKNOWLEDGMENTS

Support by the Spanish CICyT (Contract No. PB 92-0168-C), the EC (Contract No. SC1-CT91-0691), and Iberdrola S.A. is acknowledged. We also thank V. Heine, N. H. March, A. Martín-Rodero, and S. Y. Wu for helpful discussions.

[1] P. Hohenberg and W. Kohn, Phys. Rev. **136**, B864 (1964); W. Kohn and L. J. Sham, *ibid.* **140**, A1133 (1965).

[2] R. O. Jones and O. Gunnarson, Rev. Mod. Phys. **61**, 689 (1989).

[3] R. M. Dreizler and E. K. U. Gross, *Density Functional Theory* (Springer-Verlag, Berlin, 1990).

[4] D. C. Langreth and J. P. Perdew, Phys. Rev. B **21**, 5469 (1980); J. P. Perdew and A. Zunger, *ibid.* **23**, 5048 (1981).

[5] O. K. Andersen and O. Jepsen, Phys. Rev. Lett. **53**, 2571 (1984).

[6] R. Carr and M. Parrinello, Phys. Rev. Lett. **55**, 2471 (1985); **60**, 204 (1988).

[7] J. Harris, Phys. Rev. B **31**, 1770 (1985); A. P. Sutton, M. W. Finnis, D. G. Pettifor, and Y. Ohta, J. Phys. C **21**, 35 (1988); W. M. Foulkes and R. Haydock, Phys. Rev. B **39**, 12 520 (1989); O. F. Sankey and D. J. Niklewski, *ibid.* **40**, 3979 (1989); W. M. Foulkes, *ibid.* **48**, 14 216 (1993).

[8] W. A. Harrison, *Electronic Structure and the Properties of Solids* (Freeman, San Francisco, 1980).

[9] F. J. García-Vidal, A. Martín-Rodero, F. Flores, J. Ortega, and R. Pérez, Phys. Rev. B **44**, 11 412 (1991).

[10] G. Doyen, Surf. Sci. **59**, 461 (1976).

[11] C. Z. Wang, C. T. Chan, and R. M. Ho, Phys. Rev. Lett. **66**, 189 (1991); F. S. Khan and J. Q. Broughton, Phys. Rev. B **39**, 3688 (1989).

[12] F. Guinea, C. Tejedor, F. Flores, and E. Louis, Phys. Rev. B **28**, 4397 (1983).

[13] L. Hedin, in *Elementary Excitations in Solids, Molecules and Atoms*, edited by J. T. Devreese, A. B. Kunz, and T. C. Collins (Plenum, New York, 1974).

[14] L. Hedin and S. Lundqvist, in *Solid State Physics*, edited by H. Ehrenreich, F. Seitz, and D. Turnbull (Academic, New York, 1969), Vol. 23; J. Callaway and N. H. March, *Solid State Physics*, edited by H. Ehrenreich, F. Seitz, and D. Turnbull (Academic, New York, 1984), Vol. 38.

[15] A similar calculation is found in O. Gunnarsson and K. Schonhamer, Phys. Rev. Lett. **56**, 1968 (1986), where the total energy of a cluster is already obtained as a function of the orbital occupancies.

[16] D. A. Papaconstantopoulos, *Handbook of the Band Structure of Elemental Solids* (Plenum, New York, 1986).

[17] H. Ishida, Phys. Rev. B **42**, 10 899 (1990).

[18] E. Wimmer, A. J. Freeman, J. R. Hiskes, and A. M. Karo, Phys. Rev. B **28**, 3074 (1983).

[19] P. Vogl, P. Hjalmarson, and J. D. Dow, J. Phys. Chem. Solids **44**, 365 (1983).

[20] F. Manghi, C. M. Bertoni, C. Calandra, and E. Molinari, J. Vac. Sci. Technol. **21**, 71 (1982); T. U. Kampen and W. Monch (unpublished).